

THE ISOTOPE EFFECT BY ZINC DIFFUSION ALONG 43° [100] TILT GRAIN BOUNDARY IN Fe-5 at.% Si ALLOY

L.S. SHVINDLERMAN, E.I. RABKIN, B.B. STRAUMAL, L. SIEGERT* and R. VOIGTMAN*

Institute of Solid State Physics, Academy of Sciences of the URSS, Chernogolovka, Moscow district 142432, U.R.S.S.

**Zentralinstitut für Festkörperphysik und Werkstofforschung AdW der DDR, DDR-8027 Dresden, Postfach, D.R.G.*

Abstract

The distribution of stable zinc isotopes in the regions of bulk and grain-boundary diffusion of zinc in bicrystals of Fe-5 at.% Si with tilt grain boundary [100] 43° is studied by means of local secondary ion mass-spectrometry. Two-dimensional images are obtained which evidently show the existence of regions of wetting rapid diffusion (premelting region) and common diffusion on the grain boundary. The isotope effect is determined for bulk diffusion and diffusion along premelting layer for zinc isotope pairs 64/66, 64/67 and 66/67.

1. Introduction

In our previous works [1-3], we studied penetration of zinc by tilt grain boundaries [100] in alloys of iron with 5 and 6 at.% respectively. It was found that in the whole studied range of temperatures (625...908°C), liquid phase Fe-Si-Zn wets the grain boundaries. It was found that in the range of zinc concentration at grain boundary C_B from bulk solubility limit C_0 from bulk solubility limit C_{B1} to a concentration C , the measured parameter $D'\delta$ is abnormally high (here D' is the coefficient of grain boundary diffusion, δ is the diffusional thickness of grain boundary). At C_{B1} the value of product $D'\delta$ increases abruptly by roughly two orders of magnitude. We suggested that at concentration C_{B1} , grain boundary undergoes a premelting transition. In such transition, a thin thermodynamically equilibrium liquid or quasi-liquid interlayer is formed at the grain boundary [4-6]. It would be interesting to study the mechanism of zinc diffusion along the grain boundary by premelting interlayer in concentration range between C_0 and C_{B1} . The diffusion isotope effect may be measured by determination of concentration of radioactive or stable diffusant isotopes. Measuring of isotope effect by distribution of stable isotopes by the secondary ions mass-spectrometry method SIMS has great advantages [7-8].

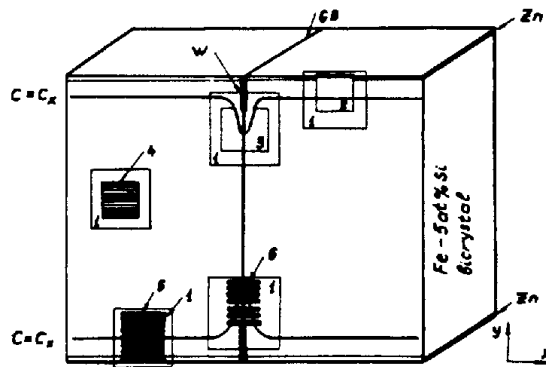


Fig.1. Fe-5 at.% Si bicrystal after diffusion anneal. GB-grain boundary; $C=C_x$ -isoconcentration line; W-wetting layer on the grain boundary; Zn-zinc layer on the sample surface. 1-presputtering area, 2-the SIMS-measurements in two-dimensional picture mode,

bulk diffusion layer; 3-the same as 2, grain boundary diffusion; 4-the raster far from surface and grain boundary for underground estimation; 5-the line scans in the bulk diffusion area; 6-the line scans along the grain boundary.

2. Experimental

The isotope effect was measured on the bicrystalline specimens of alloy Fe+5 at.% Si. Their size was $1.5 \times 1.5 \times 10 \text{ mm}^3$. These bicrystals were grown by means of electron-beam melting. The grain boundary and the specimen surface to which the diffusant was applied were orthogonal to the cross-section plane (cf. the diagram in Fig.1). The measurements of the isotope effect on bulk and grain-boundary diffusion were carried out by SIMS-microprobe IMMA (Ion Microprobe Mass Analyzer, ARL USA). The initial modification of the installation had been described in [9]. In installation located in Central Institute for Solid State Physics and Materials Science, Ac.Sci., GDR the vacuum system is modified, and, besides, it is equipped by an original computer system based on micro-computer SM-4 (USSR analogue of PDP 11/34). The isotope effect was measured by two methods (cf. Fig.1): 1. Sequential obtaining of two-dimensional images of zones of bulk and grain-boundary diffusion for various isotopes. Here, the term of obtaining one image was 10 to 50 minutes; 2 the determination of integral isotope concentration in a zone with the width equal to the primary ion beam diameter (8 to $10 \mu\text{m}$) and the length equal to $75 \dots 100 \mu\text{m}$ (line scanning mode). In such experimental layout, the concentration of isotopes of interest was determined with the interval of 16-128 secs. In the measurements, the primary beam of ions $^{16}\text{O}^+$ was used (energy 18.5 kV, beam current $\sim 1 \text{ nA}$, beam diameter $8 \dots 10 \mu\text{m}$). The reference mass-spectra measured on specimen regions far from the layers of bulk or grain-boundary diffusion and on the standard zinc specimen (natural isotope mixture) showed that the overlay of lines corresponding to zinc isotopes 66, 68, 70 with the lines of oxides $^{50}\text{Cr}^{16}\text{O}^+$, $^{52}\text{Cr}^{16}\text{O}^+$ and $^{54}\text{Fe}^{16}\text{O}^+$ (formed by bombardment of the specimen with the oxygen ions) is observed.

We studied zinc diffusion in iron matrix, so the overlay on mass 70 excluded the isotope ^{70}Zn from our consideration, because even if the artificially enriched by this mixture (20% ^{70}Zn) was used, the contribution of $^{54}\text{Fe}^{16}\text{O}^+$ oxide exceeded the contribution of $^{70}\text{Zn}^+$. Traces of chromium were present in the matrix (below 0.1 at.% according to electron-beam microprobe analysis data). Low chromium concentrations combined with low value of ratio of intensities Cr/CrO (masses 53 and 69) allowed us to use the line 66 in calculating the isotope effect. The second by significance was the hydride overlay. In our case, we were to be aware of overlays $^{67}\text{ZnH}^+ / ^{68}\text{Zn}^+$ and $^{66}\text{ZnH}^+ / ^{67}\text{Zn}^+$. But the ratios of intensities of lines 68/69 and 64/65 measured on the zinc standard specimen were

equal to 125 and 215. Thus, we safely neglected the hydride contribution.

Before measuring, the preliminary sputtering of specimen surface was always carried out. The linear size of preliminary sputtered region was roughly two times as large as that of the region where measurements were afterwards carried out. During preliminary sputtering, the concentrations of oxygen, iron chromium, and zinc were being checked. The oxygen equilibrium was obtained in 5...10 min. It was found, though, that in course of mechanical processing the sample surface was contaminated with chromium which is contained in the Wood's alloy (1...3%. Therefore, the preliminary sputtering lasted for 40...60 min because the chromium concentration acquired its steady-state level in 20-30 min.

The ratio

$$E = \frac{D_1/D_2 - 1}{(m_1/m_2)^{1/2} - 1}$$

is called the isotope effect. Here, D_1 and D_2 are the bulk diffusion coefficients, m_1 and m_2 are the atomic masses on two isotopes. To determine the relative difference between the bulk diffusion coefficients $(D_2/D_1) - 1 = \Delta_b$, a dependence of the parameter

$(C_2/C_{O_2}) - (C_1/C_{O_1})$ vs $\alpha/\sqrt{\pi} l^{\alpha^2}$ was determined. Here C_{O_1} and C_{O_2} are the isotope concentrations corresponding to the bulk solubility limit of zinc isotopes in the alloy, and $\alpha = \text{erf}^{-1}(1 - C_2/C_{O_2})$.

Parameter Δ_b is equal to the tangent of the curve in these coordinates. For calculation of the relative difference of the grain-boundary diffusion coefficients Δ_{gb} the dependence

$2 \ln \left[\frac{C_{1GB} C_{O_2}}{C_{O_1} C_{2GB}} \right]$ vs $\ln(C_{2GB}/C_{O_2})$ was determined Δ_{gb} is equal to the

sum of the tangent of this line and $1/2 \Delta_b$. Such calculation procedure follows from the nature of solutions of diffusion equations (1) and (2) used by us. Here we assume that Δ_b and $\Delta_{GB} \ll 1$, so the expansion of all functions into series with relation to Δ may be limited by the first term.

3. Results and discussion

In Figs. 2A, B we present the two-dimensional distribution of ^{64}Zn isotope in the bicrystal of Fe+5 at.% Si with tilt grain boundary [100] 43° after diffusional anneal at 735°C for 198h. Image has the size of $230 \times 230 \mu\text{m}^2$. During measurements, the beam was swept through the specimen surface by steps of $0.4 \mu\text{m}$ forming the raster of resolution 512×512 points. Therefore, craters created by primary beam were significantly overlaid, thus the surface remained practically flat after ion etching. In data processing, the subraster 4×4 was used. This means that every point of the two-dimensional image was formed by summing up the numbers of pulses obtained from 16 adjacent positions of the primary ion beam. Therefore the image contains 128×128 . This initial situation is illustrated in Fig. 2A. In Fig. 2B the same image after auxiliary processing is presented, in which random outbursts have been removed by the way of filtration. These outbursts can be seen as bright points in Fig. 2A. Besides, the brightness range had been

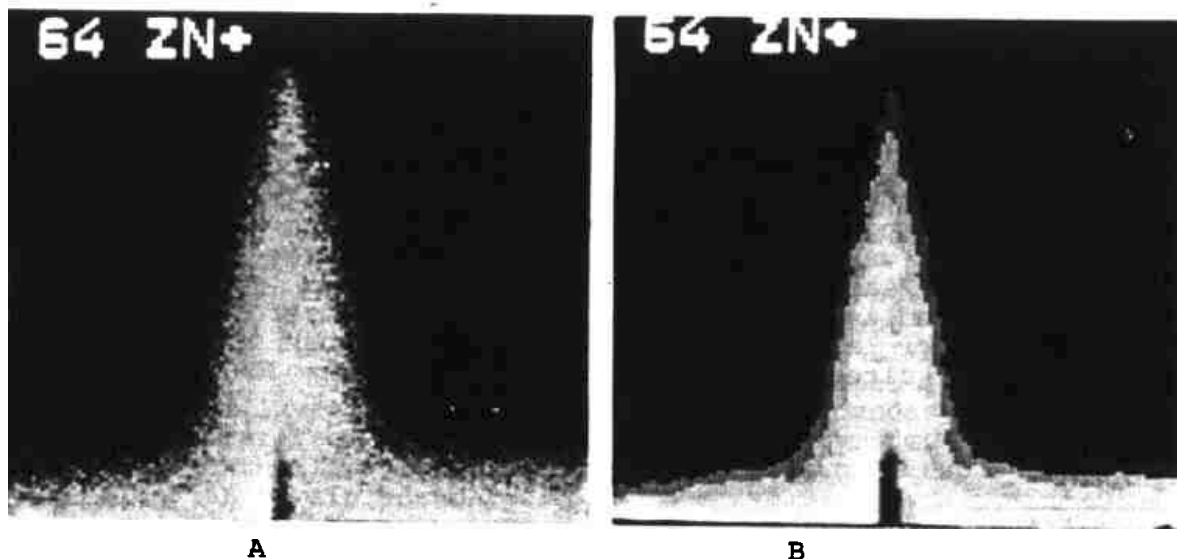


Fig.2. Distribution of zink isotopes in Fe-5 at.% Si bicrystal with tilt grain boundary [100] 43° after diffusion anneal 735°C , 198hs. $^{16}\text{O}^+$ primary ions, diameter of primary beam ca $10\ \mu\text{m}$, 512×512 pixels, $10\text{ms}/\text{pixel}$, ca $230 \times 230\ \mu\text{m}$, subraster 4×4 points, spacing between primary beam positions ca $0,4\ \mu\text{m}$, picture has 128×128 points. A- ^{64}Zn , bulk and boundary diffusion layers; B-picture from fig.2a after filtering and ranging (16 grey scale levels), the slow and fast grain boundary diffusion layers are visible.

subdivided into 16 steps. This enabled us to plot the isoconcentration contours on the image. It can be seen from Fig.2B that in the vicinity of the surface, a region of wetting exists. Isoconcentration contours in Fig.2B are chosen so that the region of rapid diffusion grain boundary beneath the wetting region is stressed. It can be seen in Figs.2B that the isoconcentration contours are nearly equidistant in the vicinity of the surface. The same distance is between two outer contours enveloping the grain boundary. In the premelting region (beneath the wetting region on grain boundary) the distance between the contours is large. Therefore it can be clearly seen from Figs.2B that the grain boundary contains the region of rapid diffusion and the region of comparatively slow diffusion.

In Fig.3 are presented the dependences of count rates I_y for zinc isotopes ^{64}Zn , ^{66}Zn , ^{67}Zn and iron isotope ^{56}Fe upon depth y_y in the layer of zinc bulk diffusion anneal at 890°C for 5h. The data were obtained by line scanning method. Each point in Fig.3 corresponded to the integral by a band of size roughly $10 \times 100\ \mu\text{m}$ (cf. Fig.1), measurement term was 16...128c. It grew as count rate for zinc isotopes decreased. The total number of pulses was, therefore, of the order of magnitude of 10^5 , and the relative error connected with the counting statistics was of the order of 10^{-3} . On the sample presented in Fig.2, the bulk diffusion region was rather narrow so the isotope effect for bulk diffusion was determined separately, on sample subjected to longer anneal. In Fig.4 are presented the dependences of I_y for the same isotopes as in Fig.3, but for the diffusion along the tilt grain boundary [100] 43° after anneal at 735°C for 198 h. Measurements were carried out in the line scanning mode. The direction of scanning was parallel to the surface and perpendicular to the grain boundary as shown in Fig.1. The value of $y_{gb} = 0$ in Fig.4 roughly corresponds to the margin of wetting zone on grain boundary (cf. Fig.2). Three regions can be distinctly seen in the figure: the premelting region (where

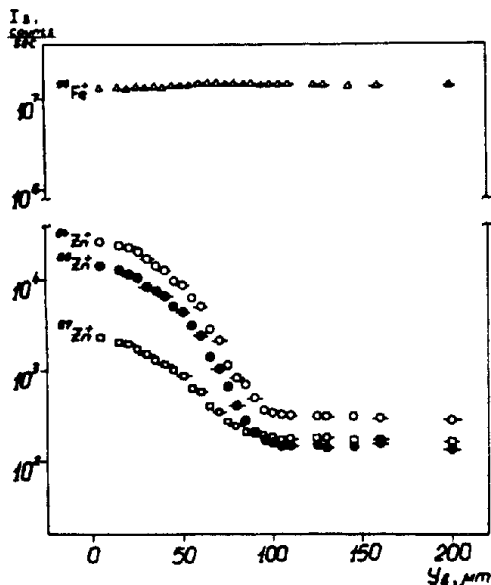


Fig.3. The iron and zinc concentrations in bulk diffusion layer (890°C, 40hs), line scan mode. I_s - count rate, y_b - the distance perpendicular to the surface with zinc layer (cf. fig.1). The counting time per point is 32-128 sec. The line scan breadth is ca 100 μm

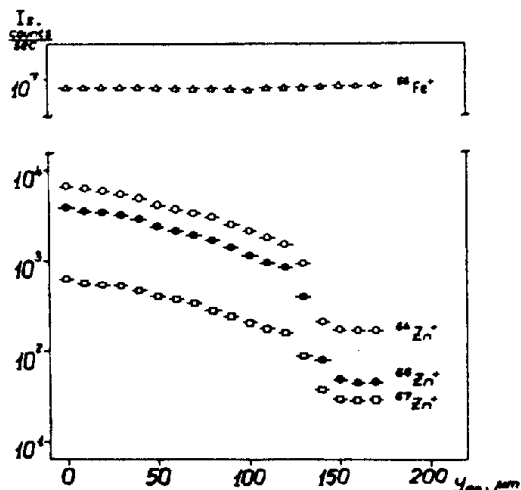


Fig.4. The iron and zinc concentrations in grain boundary diffusion layer (735°C, 198hs), line scan mode. I_s - count rate, y_{GB} - the distance along grain boundary, perpendicular to the surface of sample (cf. fig.1) $y_{GB}=0$ corresponds to the end of the wetting layer on grain boundary. The kinks on the zinc $I_s(y_{GB})$ dependences correspond to the concentration of the premelting grain boundary phase transition. The counting time per point is 16-128 sec. The line scan breadth is ca 100 μm.

Isotope effect $E = (D/D_1 - 1) / (m_1/m_2)^{1/2} - 1$

Z_1/Z_2	Bulk diffusion		Grain boundary diffusion (line scans) $\Delta_{GB} = (D_1/D_2) - 1$	$E_{GB} = (\Delta_{GB} + 0,5\Delta_b) / (m_1/m_2)^{1/2} - 1$
	2-D pictures	line scans		
64/66	1,8±0,7	1,1±0,5	0,039±0,024	3,4±1,5
64/67	1,2±0,9	0,3±0,9	0,060±0,032	3,0±1,5
66/67	0,2±2	-1,5±2,4	0,023±0,029	2,7±2,5

the zinc concentration decreases with depth slowly), the common diffusion region (where concentration decreases rapidly), and the region of noise intensity. Three zinc isotopes were used in calculations of isotope effect: ^{64}Zn , ^{66}Zn , ^{67}Zn . The estimations of contribution of $^{56}\text{Cr}^{16}\text{O}^+$ oxide show that this contribution does not exceed half of the noise intensity at large distance from the samples surface. Therefore in calculations the isotope effect by isotopes 64, 66, 67, we simply subtracted the noise intensity determined far from the sample surface. An attempt to assess and subtract the contribution of $^{56}\text{Cr}^{16}\text{O}^+$ from the intensity of line 68 lead to unacceptably big error. Therefore, line 68 was not used in calculations of the isotope effect. In calculations we took into account small difference in the probabilities of sputtering of isotopes of different atomic masses [11]. For mass difference equal

to 1, this difference was equal roughly 1,5% and very slightly affected our results. In Table are presented the values of the isotope effect determined by the data of line scanning for bulk and grain boundary. Using the two-dimensional concentration distribution we calculated intensity sum for each line of the picture parallel to the sample surface. Then the data were processed in the same way as the results of line scanning. It can be seen from the Table 1 that calculation of the isotope effect by two-dimensional pictures yields greater standard deviation than that of E calculations by results of line scanning. This, as has been noted, may be explained by the fact that the interval between measurements for different isotopes in two-dimension distributions analysis is by 1 or 2 orders of magnitude larger than that for line scanning. To calculate the isotope effect for grain boundary diffusion it is necessary to add to the Δ_{GB} value half of the Δ_b value for the bulk diffusion. This sum is presented in the fourth column of the table. It is known that for random walk, the magnitude E of the isotope effect for bulk diffusion can not exceed 1. We see that E values from the first and second columns of the table satisfy this equation provided the big standard deviation is taken into view. At the same time, the isotope effect for grain-boundary diffusion in the premelting region significantly exceeds the isotope effect for bulk diffusion. Furthermore, its values exceed 1. Therefore, values of the isotope effect for grain-boundary diffusion in premelting region and for bulk diffusion measured under identical conditions differ regressively. Big E values for grain-boundary diffusion in premelting region allow one to suggest cautiously that the excludingly high rate of grain-boundary diffusion may be accompanied by deviations from the random walk mechanism. In any case this point is worth additional experimental investigation. Particularly, it is necessary to lift the precision of the isotope effect determination. Our estimations show that error may be made smaller by roughly an order of magnitude by proper choice of the isotope mixture, the anneal conditions and the sample configuration.

REFERENCES

- /1/ Shvindlerman, L.S., Rabkin, E.I. and Straumal, B.B., Acta Metallurgica, in press.
- /2/ Shvindlerman, L.S., Rabkin, E.I., Semenov, V.N. and Straumal, B.B., Acta Metallurgica, in press.
- /3/ Łojkowski, W., Shvindlerman, L.S., Rabkin, E.I. and Straumal, B.B., this conference.
- /4/ Cahn, J.W., J.Chem.Phys., 66 (1977) 3667.
- /5/ De Gennes, P.G., Rev. of Mod.Phys., 57 (1985) 827.
- /6/ Dietrich, S., in: "Phase Transitions and Critical phenomena", ed by C.Domb and J.Lebowitz, p.1-218, v.12, Academic Press, London (1988).
- /7/ Ishioka, S. and Koiwa, M., Phil.mag.A, 52 (1985) 267.
- /8/ Södervall, U., Odelius, H., Lodding, A., Roll, U., Predel, B., Gust, W. and Dorner, P., Phil.Mag.A, 54 (1986) 539.
- /9/ Liebl, H., J.Appl.Phys., 38 (1967) 5277.
- /10/ Siegert, L. and Voigtman, R., Bild und Ton, 41 (1988) 12.
- /11/ Shimizu, N. and Hart, S.R., J.Appl.Phys., 53 91982) 1303.